Evaluation of On-state Voltage $V_{CE(ON)}$ and Threshold Voltage V_{th} for Real-time Health Monitoring of IGBT Power Modules

Mohd. Amir Eleffendi, C. Mark Johnson
University Of Nottingham
School of Electrical and Electronics Engineering
Nottingham, UK
E-Mail: eexmae@nottingham.ac.uk, eezmj@nottingham.ac.uk

Acknowledgements

The authors of this paper would like to thank the UK Engineering and Physical Sciences Research Council for funding this work through the research grants EP/I031707/1 and EP/H03014X/1.

Keywords

«Reliability», «Condition Monitoring», «Estimation Technique», «IGBT», «Measurement», «Junction Temperature», «Thermo-Sensitive Electrical Parameters».

1. Abstract

This paper investigate by experiment and simulation the use of the real-time measurements of on-state voltage $V_{CE(ON)}$ and threshold voltage V_{th} for real-time health monitoring of IGBT power modules. A study of the dependencies of each parameter on temperature, wear-out mechanisms and operating conditions is presented. Online measurement circuits are developed to obtain these two parameters during the normal operation of power converters. Junction temperature estimation for health monitoring is implemented using V_{th} which is a thermo-sensitive electrical parameter. The data of $V_{CE(ON)}$, V_{th} and T_J are combined in a residual-based health monitoring framework which allows the discrimination between dominant failure mechanisms of power module which are wire-bond liftoff and solder fatigue.

2. Introduction

IGBT power modules are widely used in many reliability critical applications. Their reliability requirements have increased over the recent years as they are used in renewable energy, transportation and aerospace applications. They have been reported as the most delicate component especially in applications with large temperature swings such as wind turbines [1]. Unpredictable failures resulting from wear-out mechanisms can have large economic implication in some applications e.g. offshore wind turbines and traction [2]. Therefore, achieving high availability of such systems is very important. Redundant power systems are one solution, but they can increase cost and complexity of power systems. Therefore, online monitoring and health management algorithms have been proposed [3-5] as an alternative solution to ensure availability and readiness of power converters in their work environment. They aim to reduce periodic maintenance, system down-time and cost through continuous monitoring of operating parameters.

Online measurement of failure indictors is essential for real-time health monitoring of power modules, for example the on-state voltage $V_{CE(ON)}$ is a common failure indictor for wire-bond lift-offs. But the difficulty of achieving accurate online measurement in addition to its small variations with degradation have limited its application in real-time health management [6]. In addition to the effect of wire-bond failure, loading and temperature variations affect $V_{CE(ON)}$ and mask the degradation content. Therefore, the masking effects of those factors should be separated from degradation effect, so that the underlying health information can be extracted. Junction temperature T_J on the other hand

is considered to be an indicator of thermal degradation [7]. However, obtaining junction temperature of an IGBT module in real-time is difficult.

Multiple approaches are proposed to measure or estimate junction temperature in real-time e.g. integrated sensor [8], model-based estimates [9] and thermo-sensitive electrical parameters (TSEPs) [10, 11]. TSEPs appear to be a promising approach since it is non-invasive and it uses the IGBT chip itself as the temperature sensor. Among the multiple TSEPs available, threshold voltage V_{th} shows good correlation with temperature. However, in filed operating conditions, noise from working environment of power converters can degrade measurement accuracy and increase measurement error. This consequently has an effect on the accuracy of the estimated junction temperature. Therefore, achieving an accurate junction temperature estimate is very important to enable health monitoring of power module.

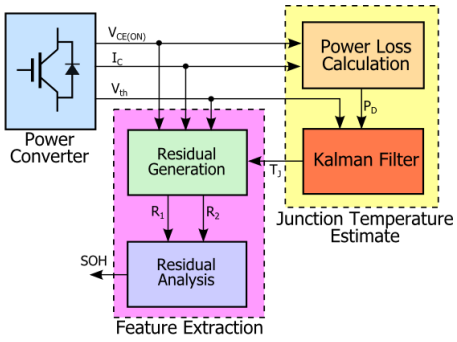

Figure 1. Real-time Health monitoring of IGBT power modules.

This paper explains through experiment and simulation that using online measurements of failure indicators of $V_{CE(ON)}$ and T_J allows distinguishing between dominant failure mechanisms of power modules (wire-bonds and solder fatigue). This can be accomplished through the proposed framework shown in Figure 1. Measurements of loading current I_L, $V_{CE(ON)}$ and V_{th} are made on the power converter for the monitored IGBT. On-state voltage $V_{CE(ON)}$ and loading current I_L are used to calculate the power loss of the IGBT. It is then used with threshold voltage V_{th} which is a TSEP to estimate junction temperature T_J with improved accuracy through the algorithm of Kalman Filter [12]. Health monitoring is then achieved by residual generation and analysis where estimated T_J and measurements of I_L, $V_{CE(ON)}$ and V_{th} are all combined to separate operating conditions and extract packaging degradation features.

3. Online Measurement of On-state Voltage $V_{CE(ON)}$

3.1. Temperature and Wire-bond Failure Effects on $V_{CE(ON)}$

The relationship between $V_{CE(ON)}$ and temperature is dependent on current and has a nonlinear temperature coefficient. Figure 2 shows the I-V characteristic of 1.2kV/400A IGBT module at multiple temperatures which describes that relationship. It is clear that the temperature coefficient of $V_{CE(ON)}$ is a non-linear function of current; at low currents $V_{CE(ON)}$ has a negative temperature coefficient and at high currents it has a positive temperature coefficient. The point where temperature coefficient changes sign is the inflection point and here $V_{CE(ON)}$ becomes independent of temperature. For the example module under test, the negative temperature coefficient of $V_{CE(ON)}$ below inflection point is found to have a maximum value of 1.23mV/^{o}C at 8A which decreases in magnitude towards inflection point. Above that point the temperature coefficient becomes positive and increases with current to reach 2.68mV/^{o}C at 180A.

Figure 3 shows varaition of $V_{CE(ON)}$ with number of wire-bonds attached. A single-chip IGBT module is used for this test where wires were deliberatly cut and I-V curves obtained. It is clear from

Figure 2 and Figure 3 that temperature and wire-bond failures affect $V_{CE(ON)}$ in the same manner. Hence, the masking effect of temperature on $V_{CE(ON)}$ hides the effect of wire-bond failure and it is important to remove this masking effect for efficient real-time health monitoring.

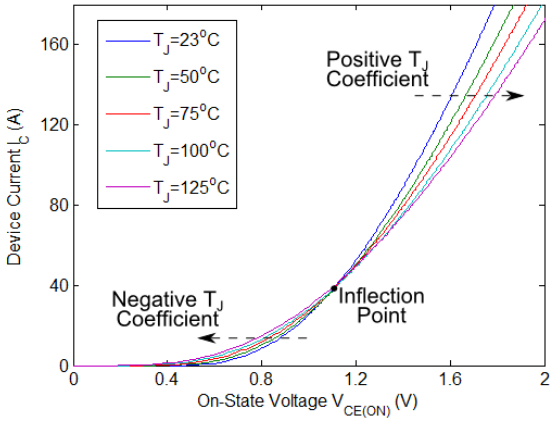

Figure 2. I-V characteristic of a 1.2kV/400A IGBT power module at multiple temperatures explains temperature dependency of the on-state voltage $V_{CE(ON)}$.

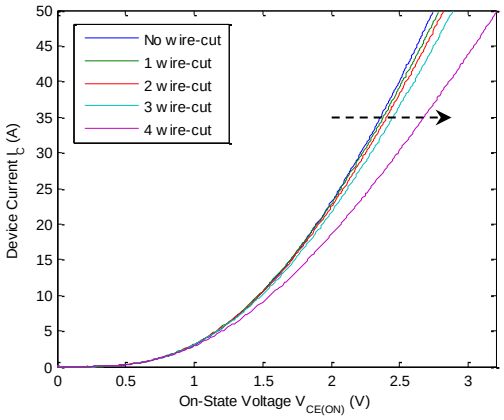

Figure 3. I-V characteristic of a single-chip IGBT module shows change of $V_{CE(ON)}$ with wire-bond attached.

3.2.Measurement Circuit

Online measurement of the on-state voltage $V_{CE(ON)}$ for temperature estimation, during normal operation of power converters, can be a challenge. The voltage across the IGBT device has a wide dynamic range (between DC link voltage and on-state voltage) and must be captured with millivolt resolution and accuracy. Precise timing, synchronized to the device switching instants, is required in order to capture a consistent representation of $V_{CE(ON)}$. In addition, electrical isolation is required between power converter and the processing end point to eliminate current loops and achieve safety. Therefore, a dedicated measurement circuit is developed to meet these requirements. Figure 4 shows the functional block diagram of the measurement circuit.

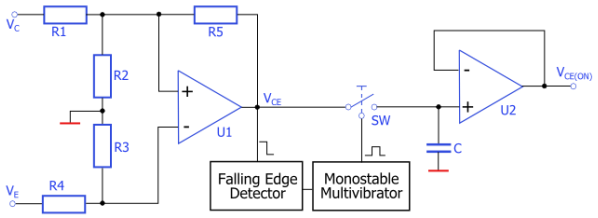

Figure 4. A block diagram of the online measurement circuit of $V_{CE(ON)}$

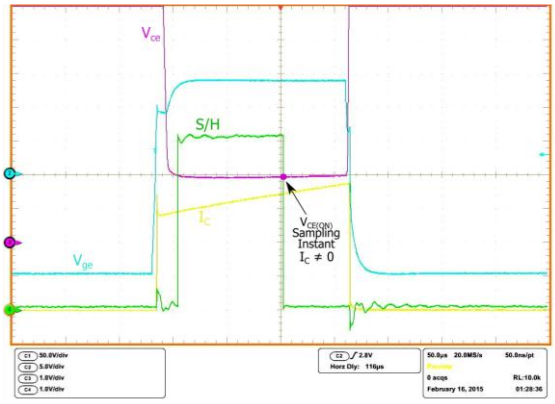

Figure 5. Double pulse test shows waveforms of current I_C gate-emitter voltage V_{ge}, collector-emitter voltage V_{CE} and sampling signal S/H

A differential amplifier U1 is used to capture the collector-emitter voltage V_{CE} across the IGBT device. The amplifier output goes into a timing circuit, a falling edge detector and a monostable multivibrator generate a sample and hold (S/H) signal. The S/H circuit picks up a sample of V_{CE} 100us after the falling edge of the transient in V_{CE}, so giving enough time for this value to stabilize. This time should be chosen according to the switching frequency. This is done by appropriate choice of component values. A capacitive isolator is used to provide electrical isolation between the power

converter and the measurement end point. Every switching cycle, a single sample of $V_{CE(ON)}$ is captured and held until the next switching cycle. The operation of the circuit is tested in a double pulse tester. Figure 5 shows the operating waveforms of the measurement circuit during a normal switching cycle.

4. Online measurement of Threshold voltage V_{th}

4.1. Temperature dependency

Threshold voltage is the minimum V_{GE} voltage required to form an inversion layer at the interface between the substrate region and the gate oxide at the MOS-structure in the IGBT. This inversion layer constitutes a conducting channel that allows the collector current to pass from collector to emitter. It can be described by the following expression [13]:

$$V_T = V_{FB} + 2\Psi_B + \frac{\sqrt{4\varepsilon_S q N_A \Psi_B}}{C_{OX}}$$

where V_{FB} is the flat-band voltage, q is the elementary charge of the electron. ε_S is the silicon dielectric constant, N_A is the doping concentration C_{OX} is the capacitance of the oxide and ψ_B is the bulk potential. Threshold voltage can be extracted from the transfer characteristic of the IGBT [14]. The threshold voltage is defined as the x-intercept of the tangent of the I_{CE}-V_{GE} curve as explained in Figure 6. That is, it is the voltage at which the tangent intersects with I_{CE}=0. The IGBT module is mounted on a temperature controlled hot plate and the transfer characteristic is obtianed at muliple temperartures.Figure 6 shows the square-root of I_{CE} as a function of V_{GE} of the 1.2kV/400A IGBT module at multiple temperatures. Figure 7 shows the extracted threshold voltage as a function of temperature.

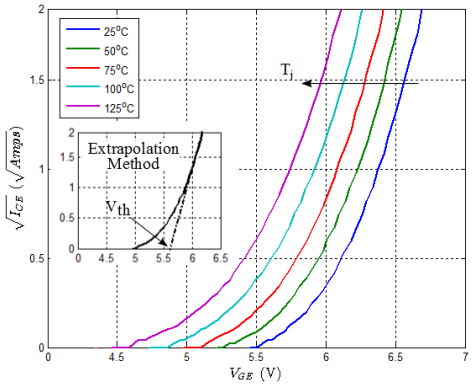

Figure 6. square-root of current vs. V_{GE} shows variation of threshold voltage at multiple temperatures of 1.2kV/400A IGBT module.

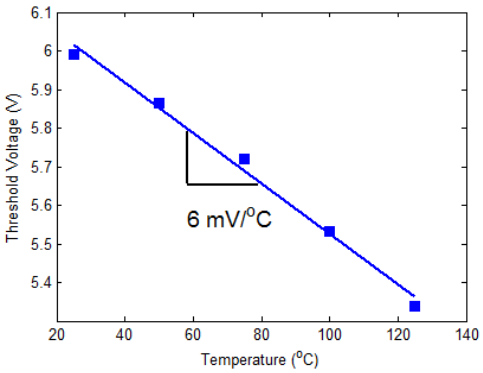

Figure 7. Variation of threshold voltage V_{th} with temperature as extracted from the transfer characteristic.

It is clear that the threshold voltage has a linear relasionship with temperature. The temperature coefficient is found to be -6mV/°C for the module under test. In general, this coefficient depends on the semicondutor device and ranges between -2mV/°C to -10mV/°C [10]. Those characteristics of linearty and relatively high sensitivity to temperature make it a good candidate as a thermo-sensitive parameter TSEP in comparison to other parameters.

In addition to its temperature dependency, it is known (see for example Sze [15]) that threshold voltage has dependence to collector-emitter voltage. It is described that the application of a voltage across the substrate region of the IGBT induces a change in the oxide potential at the gate. This changes the width of the depletion layer which consequently changes the charge of the depletion region. Therefore, the threshold voltage is going to be shifted under a biased substrate by the amount [15]:

$$\Delta V_T = \frac{\sqrt{2\varepsilon_S q N_A}}{C_{OX}}\left(\sqrt{2\Psi_B - V_{BS}} - \sqrt{2\Psi_B}\right)$$

4.2.Measurement circuit

For the online measurement of V_{th} the measurement circuit shown in Figure 8 is developed. The working principle of the circuit follows the work in [16].V_{GE} is obtained using the voltage dividers formed of R1-R2 and R3-R4. The capacitors are used to improve the frequency response of the voltage divider. An instrumentation amplifier U1 is used to obtain the differential voltage V_{GE}. In order to detect the current initiation, the voltage drop across the parasitic inductance of the auxiliary emitter is used. The comparator U3 is a high speed comparator. It triggers the track and hold circuit to capture the value of V_{GE} at the current initiation instant by comparing the voltage drop across the emitter parasitic inductance to a reference voltage V_{ref}. When the gating signal is applied to the IGBT gate, the track and hold circuit operates in the tracking mode and the capacitor C5 follows V_{GE}. At the instant of current initiation the output of the comparator U3 changes state and triggers the switch SW, which opens and the capacitor holds the value of V_{GE}. The captured value is a good estimate of the threshold voltage V_{th}. This is descried in Figure 9 where the measurement circuit is tested in a double pulse tester.

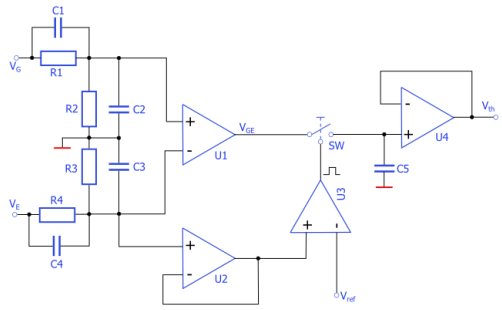

Figure 8. The online measurement circuit of threshold voltage

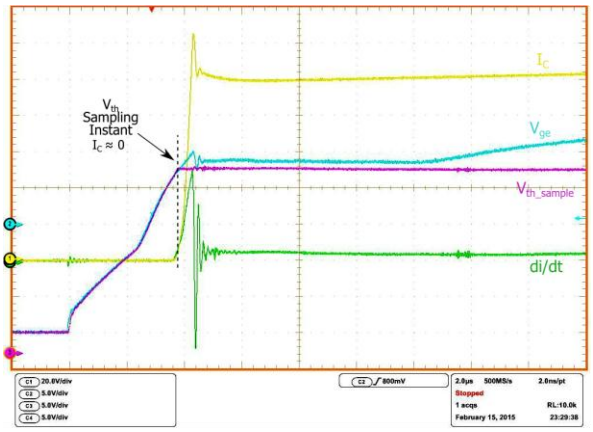

Figure 9. Operating waveforms of V_{th} measurement circuit during a normal switching cycle of an IGBT. Device current (I_C), gate-emitter voltage (V_{ge}), di/dt measured across parasitic inductance (di/dt) and measured V_{th} ($V_{th\ sample}$)

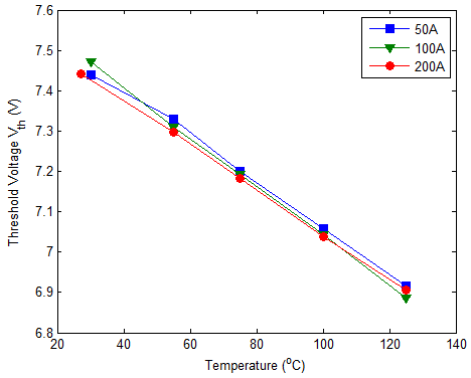

Figure 10. Calibration of threshold voltage with temperature in a double pulse test. Threshold voltage V_{th} is measured using the proposed circuit.

To validate the measurement with temperature, the IGBT module is mounted on a temperature controlled hot plate and the threshold voltage is obtained at multiple temperatures using the proposed

circuit. The calibration curves are shown in Figure 10. It can be seen that the measured V_{th} voltage is higher than the lab measured value shown in Figure 7. This can be explained by the response time of the measurement circuit (between the start of the current rise and the operation of the track and hold sample gate) which is around 15ns, in addition to the offset of the op-amps used in the circuit. However, the temperature coefficient of -6mV/^{o}C and the current independence are preserved.

The effect of wire-bond failures on V_{th} is investigated by Zhou et al [17]. He showed by experiment that V_{ge} signal has no correlation to wire-bond failures during IGBT turn-on. An observable change can be seen only after a complete failure of the IGBT chip when all emitter wire-bonds are lifted off.

5. Real-time Estimate of Junction Temperature T_J using V_{th}

As explained earlier, junction temperature is a key indicator of thermal degradation of power modules. Therefore, in order to enable health monitoring of thermal path, an accurate estimate of T_J is essential. Resolving T_J information from measurement of TSEPs can be challenging due to many reasons: the low sensitivity to T_J, dependence on loading conditions and measurement inaccuracies. Those inaccuracies originate from harsh working environment of power converters where switching and modulation signals and EMI increase measurement errors. Therefore, the algorithm of Kalman filter is used to produce an accurate estimate of T_J and eliminate the noise based on an estimate obtained from a V_{th}. On-state voltage $V_{CE(ON)}$ is a TSEP as well and can be used instead.

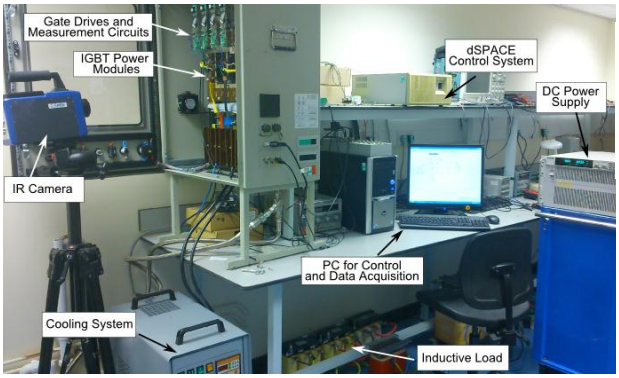

Figure 11. Experimental setup of the full-bridge inverter used to validate the real-time estimate of junction temperature T_J.

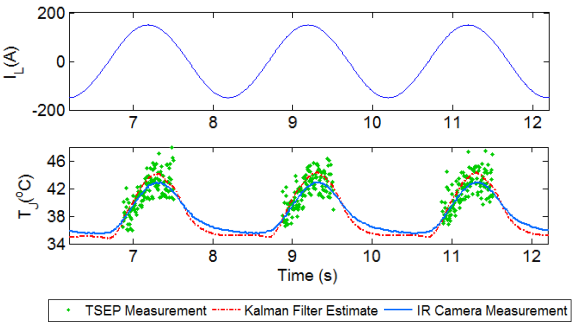

Figure 12. Experimental real-time measurements of loading current I_L and the corresponding T_J measurement from TSEP and IR Camera compared to the T_J estimate given by Kalman Filter.

Kalman filter [12] is an adaptive model-based approach that uses a thermal model of the heat conduction path to process the T_J measurements resulting from a TSEP. As shown earlier in Figure 1, a power loss model, based on the measured current, is used to calculate power dissipation which is then used as an input to the Kalman filter. The algorithm is implemented practically on a single-phase Full-bridge inverter. The test setup is shown in Figure 11. Figure 12 shows the real-time estimate of T_J produced by Kalman filter compared with Infrared camera measurement and T_J measurement from V_{th}. The improvement in T_J estimate accuracy compared to TSEP measurement is clear and it is in good agreement with Infrared camera measurement. For further details about Kalman Filter and its practical implementation the reader is referenced to the work in [18].

6. Health Monitoring of IGBT Modules by Residuals Evaluation

Residuals are defined as quantities that represent the discrepancy between measured variables and their expected values under a healthy baseline state. The expected values are obtained from models that represent the power module in its original health state. Therefore, residuals are ideally unbiased zero-valued indicating matching between actual power module and its healthy baseline model. The appearance of a bias in the residual is indicative of a deviation of the power module from its original

state. After residuals are calculated, their statistical properties are evaluated to reveal any deviation from zero. Residuals can be obtained using different methods [19]. In this work, two residuals are generated. Kalman Filter used for T_J estimation is also used as a residual generator to monitor the health state of the thermal path in a power module. Whereas a static model [20] of the IGBT forward characteristic is used for residual generation to monitor wire-bond failures.

In order to study the behaviour of residuals with package degradation, a MATLAB/Simulink model of an IGBT module is used. The model is depicted in Figure 12. The model describes the electro-thermal behaviour of an IGBT module. The forward characteristics of the IGBT and the freewheeling diode form the electrical model and they are represented by look-up tables. Those forward characteristics are functions of temperature T_J. The foreword voltage drops of the IGBT and the diode are the outputs $V=[V_{CE(ON)}, V_F]$ of the electrical model. The thermal model is a representation of the junction-to-ambient thermal impedance Z_{thja} of the IGBT module. It is modelled using a Foster network. The thermal self-heating and cross-coupling effects between the IGBT and the freewheeling diode are accounted for in the modelling. The outputs of the thermal model are the IGBT and diode junction temperatures. The input of the thermal model is the power dissipated in the module. This is calculated using a power loss model which involves the switching and conduction losses of the IGBT in addition to the reverse recovery and conduction losses of the freewheeling diode.

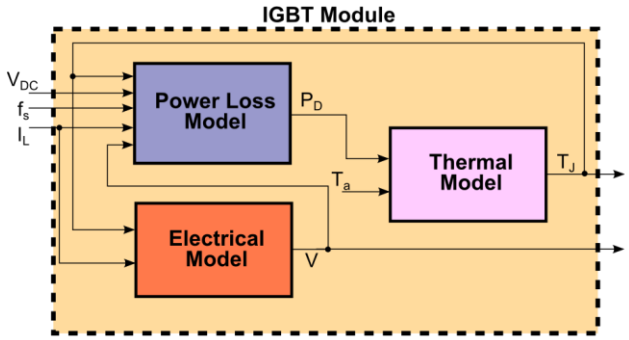

Figure 13. The electro-thermal model of the IGBT module used to study residuals behavior with packaging degradation

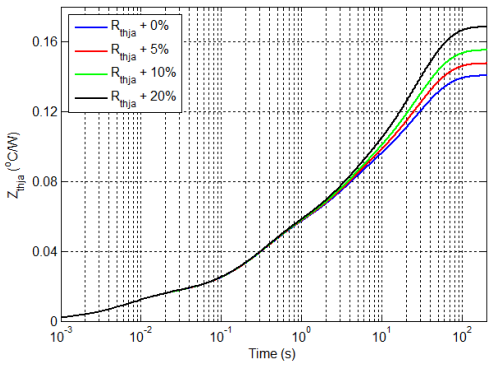

Figure 14. Simulated Thermal Impedances for baseline case (R_{thja}+0%) and degraded cases (5%, 10% and 20%)

6.1. Residual Evaluation for Thermal Degradation

Thermal degradation resulting from solder fatigue can be simulated by manipulating the parameters of the Foster network that characterizes the thermal impedance of the IGBT module. An increment of 20% in the thermal resistance R_{thja} is a common failure criteria [21, 22]. Figure 13 shows the simulated junction-to-ambient thermal impedance Z_{thja} for four cases: the original thermal impedance (R_{thja} + 0%) which represents the baseline case in addition to three degraded cases indicated by (R_{thja} + 5%), (R_{thja} + 10%) and (R_{thja} + 20%) where the junction-to-ambient thermal resistance is increased by 5%, 10% and 20% from its original value R_{thja}=0.14°C/W.

The residual used to monitor the health state of the thermal path is generated as the difference between the measurement of T_J obtained from V_{th} (T_{J_TSEP}) and the estimate produced by Kalman filter $\hat{T}_J$. The residual $r_1(k)$ at the time instant k is therefore calculated as:

$$r_1(k) = T_{J\_TSEP}(k) - \hat{T}_J \ \ (k)$$

Under ideal conditions where the thermal model is in agreement with the actual thermal path, the residual is zero-mean white noise signal. When the actual thermal path deviates from its original state characterized by the thermal model, the residual start to deviate from its zero-mean white noise properties. Therefore, the residual is tested statistically for its mean and standard deviation. These statistics are normally evaluated in a finite time window of a specific length. The size of the window

does not affect the detection speed since the thermal degradation is a slow evolving process whereas residual evaluation can be done periodically using a windows size of few seconds.

Figure 14 shows the calculated mean and standard deviation of the residual. At the baseline case (R_{thja}+0%) the mean value is approximately 0 indicating a matching between the simulated baseline thermal model and the Kalman filter. When the thermal model is change and thermal resistance is increased, a corresponding increment in the mean value and standard deviation of the residual $r_1(k)$ can be noticed indicating a deviation of the actual thermal path from its original state.

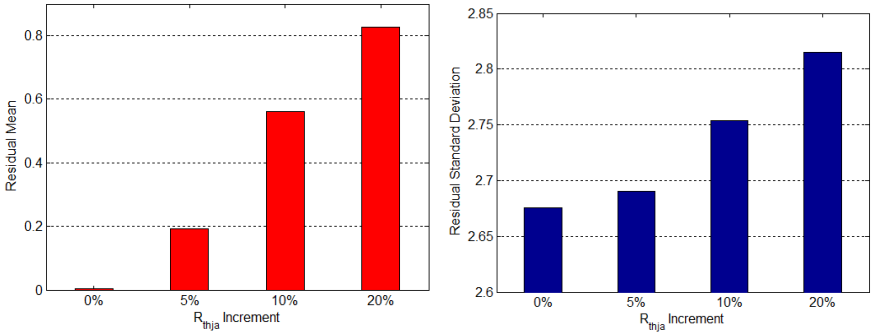

(a) (b)

Figure 15. Change of Residual Statistics as a result of thermal degradation. Mean (a) and Standard Deviation (b) both increase with increasing thermal resistance R_{thja}

6.2. Residual Evaluation for Wire-bond Failures

It is common that the wire-bond failures result in a step-wise change in the on-state voltage $V_{CE(ON)}$. A threshold for power module failure by wire-bond liftoff is generally defined by an increment of 5% in $V_{CE(ON)}$ as observed from power cycling test [6, 21]. Therefore, the wire-bond failure is simulated as an additive shift to $V_{CE(ON)}$ which is the output of the forward characteristic model of the IGBT.

The residual $r_2(k)$ is defined as the difference between the actual $V_{CE(ON)}$ that can be measured from the IGBT using the measurement circuit explained earlier and the estimated $\hat{V}_{CE(ON)}$:

$$r_2(k) = V_{CE(ON)}(k) - \hat{V}_{CE(ON)}(k)$$

where the estimated $\hat{V}_{CE(ON)}$ can be obtained from a static model of the forward characteristic of the IGBT module $V_{CE(ON)}=f(I_L,T_J)$. The measurement of the loading current I_L and the estimate of junction temperature T_J can be used to recalculate the expected value of $\hat{V}_{CE(ON)}$. Under normal condition with no wire-bond lift-offs, the residual $r_2(k)$ have the value of zero since the measured $V_{CE(ON)}$ matches the model estimated $\hat{V}_{CE(ON)}$. Any change in $r_2(k)$ from its zero value can then be correlated to wire-bonds failures.

Figure 15(a) shows a simulation of wire-bond lift-offs which happens during the normal operation of a single-phase inverter. Each liftoff is simulated by a step increment in $V_{CE(ON)}$ by 10mV which is 0.56% from its original value. It is difficult to detect such small changes in $V_{CE(ON)}$ as it is a function of loading current and temperature. That is, the changes in $V_{CE(ON)}$ due wire-bond lift-offs are masked by operating conditions. The advantage of using the residual is to remove the masking effect and reveal changes in $V_{CE(ON)}$ that result from packaging degradation. This can be seen in Figure 15(b) where the residual $r_2(k)$ is about 0 when there is no lift-off indicating a match between measured and estimated $V_{CE(ON)}$. When the lift-off failure happens at 450s and 460s the step in the residual can be clearly seen whereas it cannot be spotted in Figure 15(a).

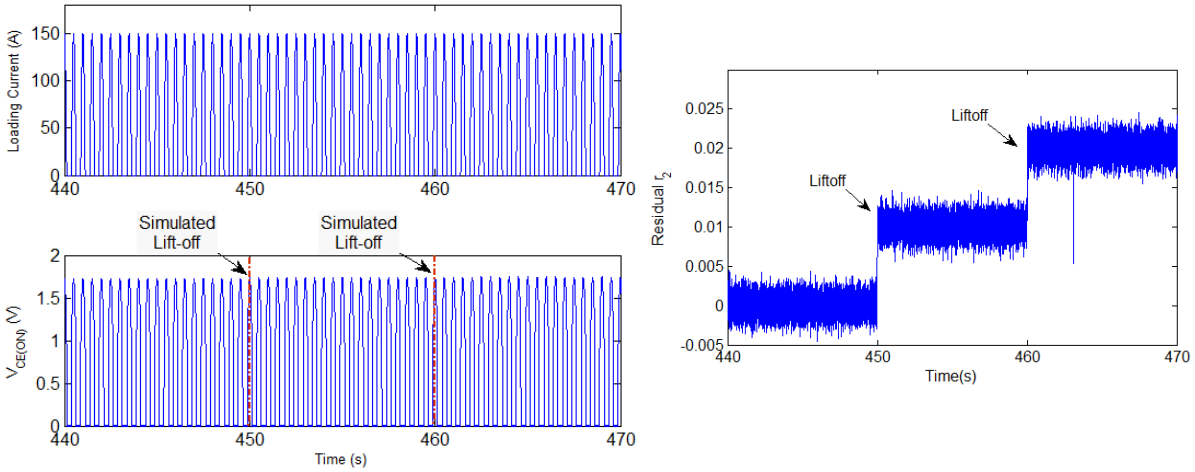

(a) (b)

Figure 16. (a) Simulated IGBT loading current and $V_{CE(ON)}$ in a single phase inverter during wire-bond lift-offs. It is difficult to detect changes in $V_{CE(ON)}$ due to masking effect of operating conditions. (b) The residual $r_2(k)$ removes masking effects and reveals changes in $V_{CE(ON)}$ resulting from wire-bond failures.

7. Future Work

The health monitoring framework presented in this paper will be tested experimentally. A preparation for a power cycling test is ongoing to validate the simulation results presented earlier. Integrating the measurement circuitry and the proposed health monitoring into gate drives is under investigation. This integration can improve availability and reliability of power converters by detection of ongoing degradation of power modules which can enable predictive maintenance.

8. Conclusion

This paper has demonstrated that real-time measurements of on-state voltage $V_{CE(ON)}$, threshold voltage V_{th} and junction temperature T_J can enable real-time health monitoring of IGBT modules. A data acquisition system has been developed to collect online measurements of these parameters during the normal operation of power converters. Experimental results are presented for the real-time measurement of $V_{CE(ON)}$, V_{th} and T_J in a single-phase full-bridge inverter. The use of these measurements for health monitoring is demonstrated through simulation. It is demonstrated that the discrimination between wire-bond failures and thermal degradation is possible by the proper combination of real-time measurements.

The proposed framework for health monitoring of IGBT modules is based on the use of residuals which are defined as the difference between actual measurements and expected values of failure indicators such as T_J and $V_{CE(ON)}$. Residuals allow removing the masking effect of operating conditions of the power converter on the failure indicator which reveals effects of packaging failures and allows detecting health degradation. Two residuals are generated to monitor the state of the thermal path and the wire-bonds. The analysis of generated residuals allows extracting the health state of IGBT power modules in real-time without the need to interrupt the normal operation of power converters.

9. References

[1] K.H. Michael Wilkinson, Ben Hendriks, Measuring Wind Turbine Reliability: Results of the ReliaWind Project, European Wind Energy Conference 2011, Brussels.

[2] Y. Shaoyong, A. Bryant, P. Mawby, X. Dawei, R. Li, P. Tavner, An Industry-Based Survey of Reliability in Power Electronic Converters, IEEE Transactions on Industry Applications, 47 (2011) 1441-1451.

[3] J.M. Anderson, R.W. Cox, On-line condition monitoring for MOSFET and IGBT switches in digitally controlled drives, Energy Conversion Congress and Exposition (ECCE), 2011 IEEE2011, pp. 3920-3927.

[4] X. Dawei, L. Ran, P. Tavner, Y. Shaoyong, A. Bryant, P. Mawby, Condition Monitoring Power Module Solder Fatigue Using Inverter Harmonic Identification, IEEE Transactions on Power Electronics, 27 (2012) 235-247.
[5] X. Dawei, R. Li, P. Tavner, A. Bryant, Y. Shaoyong, P. Mawby, Monitoring Solder Fatigue in a Power Module Using Case-Above-Ambient Temperature Rise, IEEE Transactions on Industry Applications, 47 (2011) 2578-2591.
[6] S. Yang, D. Xiang, A. Bryant, P. Mawby, L. Ran, P. Tavner, Condition Monitoring for Device Reliability in Power Electronic Converters: A Review, IEEE Transactions on Power Electronics, 25 (2010) 2734-2752.
[7] A.J. Yerman, J.F. Burgess, R.O. Carlson, C.A. Neugebauer, Hot Spots Caused by Voids and Cracks in the Chip Mountdown Medium in Power Semiconductor Packaging, IEEE Transactions on Components, Hybrids, and Manufacturing Technology, 6 (1983) 473-479.
[8] E.R.M. John F. Donlon, Takashi Igarashi, Mitsuhara Tabata, Takahiro Inoue, High Performance Intelligent Power Modules Using CSTBT Chips with Integrated Temperature Sensor, Power Electronics Technology Conference 20032003.
[9] M. Musallam, C.M. Johnson, Real-Time Compact Thermal Models for Health Management of Power Electronics, IEEE Transactions on Power Electronics, 25 (2010) 1416-1425.
[10] Y. Avenas, L. Dupont, Z. Khatir, Temperature Measurement of Power Semiconductor Devices by Thermo-Sensitive Electrical Parameters: A Review, IEEE Transactions on Power Electronics, 27 (2012) 3081-3092.
[11] S.H. Hiller, C; Lutz, J, Measurement of Tvj in a B6 IGBT inverter for electric vehicles using the Vce(T)-method Proceedings of the 12th Inernational Seminar on Power Semiconductors ISPS'142014, pp. 81-84
[12] M.S. Grewal, A.P. Andrews, Kalman Filtering: Theory and Practice Using MATLAB, Wiley2011.
[13] B.J. Baliga, Power Semiconductor Devices, Wadsworth Publishing Co Inc1995.
[14] B.J. Baliga, Temperature behavior of insulated gate transistor characteristics, Solid-State Electronics, 28 (1985) 289-297.
[15] K.K.N. Simon M. Sze, Physics of Semiconductor Devices, 3 ed., John Wiley & Sons2006.
[16] I.Č. Bahun, Neven; Jakopović, ŽEljko, Real-Time Measurement of IGBTs Operating Temperature, Automatika: Journal for Control, Measurement, Electronics, 52 (2011).
[17] L. Zhou, S. Zhou, M. Xu, Investigation of gate voltage oscillations in an IGBT module after partial bond wires lift-off, Microelectronics Reliability, 53 (2013) 282-287.
[18] A. Eleffendi, C.M. Johnson, Application of Kalman Filter to Estimate Junction Temperature in IGBT Power Modules, IEEE Transactions on Power Electronics, PP (2015) 1-1.
[19] J.Gertler, Analytical redundancy methods in fault detection and isolation - survey and synthesis, IFAC Fault Detection, Supervision and Safety for Technical Processes, Baden-Baden, Germany, 1991, pp. 9-21.
[20] R. Isermann, Supervision, fault-detection and fault-diagnosis methods — An introduction, Control Engineering Practice, 5 (1997) 639-652.
[21] A. Hamidi, N. Beck, K. Thomas, E. Herr, Reliability and lifetime evaluation of different wire bonding technologies for high power IGBT modules, Microelectronics Reliability, 39 (1999) 1153-1158.
[22] G. Coquery, R. Lallemand, Failure criteria for long term Accelerated Power Cycling Test linked to electrical turn off SOA on IGBT module. A 4000 hours test on 1200A–3300V module with AlSiC base plate, Microelectronics Reliability, 40 (2000) 1665-1670.